

Chemisorption of Gold(III) from Solutions Using Thallium(I) Diisobutyldithiocarbamate: Supramolecular Structure and Thermal Behavior of the Polymeric Gold(III)–Thallium(III) Complex $[\text{Au}\{\text{S}_2\text{CN}(\text{iso-C}_4\text{H}_9)_2\}_2][\text{TiCl}_4]_n$

A. V. Ivanov^{a,*}, O. A. Bredyuk^a, O. V. Loseva^a, and T. A. Rodina^b

^a Institute of Geology and Nature Management, Far East Branch, Russian Academy of Sciences, Blagoveshchensk, 675000 Russia

^b Amur State University, Blagoveshchensk, 675027 Russia

*e-mail: alexander.v.ivanov@chemist.com

Received July 2, 2014

Abstract—Chemisorption of gold(III) from 2 M HCl using thallium(I) diisobutyldithiocarbamate via an ion exchange/redox process gives a polymeric gold(III)–thallium(III) complex of the formula $[\text{Au}\{\text{S}_2\text{CN}(\text{iso-C}_4\text{H}_9)_2\}_2][\text{TiCl}_4]_n$ (**I**). Its supramolecular structure determined by X-ray diffraction (CIF file CCDC no. 1009388) comprises three structurally nonequivalent complex cations $[\text{Au}\{\text{S}_2\text{CN}(\text{iso-C}_4\text{H}_9)_2\}_2]^+$ (A, B, and C) and two nonequivalent $[\text{TiCl}_4]^-$ anions, both the cations and the anions being conformers. The isomeric cations are united through pairs of relatively weak secondary nonvalent Au–S contacts into zigzag polymer chains ($\cdots\text{A}\cdots\text{B}\cdots\text{C}\cdots\text{B}\cdots\text{A}\cdots$), with alternating nonequivalent $[\text{TiCl}_4]^-$ anions on both sides. The thermal behavior of complex **I** was studied by simultaneous thermal analysis. The TG curve shows two steps of its weight loss. The first step involves thermal decomposition of the dithiocarbamate portion of the complex and $[\text{TiCl}_4]^-$ with reduction of gold(III) to metallic gold and release of TiCl . The second step is due to evaporation of TiCl . The final thermolysis product of complex **I** is reduced metallic gold.

DOI: 10.1134/S1070328415020025

INTRODUCTION

Dialkyldithiocarbamate complexes are widely used in extraction-photometric determination of thallium(I) [1]. The toxic effect of thallium(I) compounds on living organisms is due to the formation of strong Tl–S bonds between thallium(I) and sulfur-containing groups of proteins, which blocks the biological activity of thiol-containing enzymes. This has led to growing recent interest in sulfur-containing compounds capable of efficiently binding thallium into water-insoluble stable forms. For coordination chemistry, thallium(I) dithiocarbamates are of interest because their central metal atom has high coordination numbers (C.N. 5, 6, and 7). A single ligand cannot provide coordinative saturation to the metal, so thallium(I) dithiocarbamates dimerize to form dinuclear structures $[\text{Tl}_2(\text{Dtc})_2]$ (Dtc is an appropriate dialkyldithiocarbamate anion, $\text{R}_2\text{CN}(\text{S})\text{S}^-$); supramolecular self-organization of these dimers gives rise to polymeric structures [2–8]. In addition, thallium dithiocarbamates are of practical interest as precursors to nanocrystalline thallium sulfide [9].

Earlier, we have reported on the ability of thallium(I) dialkyldithiocarbamates to bind copper(II) from solutions, yielding trinuclear copper(II)–thallium(I) complexes of the formula $[\text{CuTl}_2(\text{Dtc})_4]$ [6,

10]. Since the cadmium and zinc dithiocarbamates studied earlier can bind gold(III) from solutions to form gold(III)–cadmium [11–13] and gold(III)–zinc complexes [14, 15] with complicated structures, the synthesis of novel heteropolynuclear gold(III)–thallium complexes and investigations of their structural organization and spectral and thermal properties are of considerable interest.

In this work, we studied a reaction of polymeric thallium(I) diisobutyldithiocarbamate with the $[\text{AuCl}_4]^-$ anions in 2 M HCl. Chemisorption of gold(III) accompanied by a redox process yielded a heteropolynuclear gold(III)–thallium(III) complex of the formula $[\text{Au}\{\text{S}_2\text{CN}(\text{iso-C}_4\text{H}_9)_2\}_2][\text{TiCl}_4]_n$ (**I**). Complex **I** was preparatively isolated and examined by ^{13}C MAS NMR spectroscopy, X-ray diffraction, and simultaneous thermal analysis.

EXPERIMENTAL

Sodium diisobutyldithiocarbamate was prepared from carbon disulfide (Merck) and diisobutylamine (Aldrich) in a basic medium [1]; the original polymeric thallium(I) complex was synthesized as described in [2]. Both these compounds were addi-

tionally characterized by ^{13}C MAS NMR spectroscopy (δ , ppm):

$\text{Na}\{\text{S}_2\text{CN}(iso\text{-C}_4\text{H}_9)_2\} \cdot 3\text{H}_2\text{O}^*$ δ : (1 : 2 : 2 : 4): 208.2 ($-\text{S}_2\text{CN}=$); 66.7 ($=\text{NCH}_2-$); 28.0, 27.1 (1 : 1 : $=\text{CH}-$); 23.0, 22.4, 20.8 (1 : 1 : 2, $-\text{CH}_3$). $[\text{Tl}_2\{\text{S}_2\text{CN}(iso\text{-C}_4\text{H}_9)_2\}_2]_n$ (**II**): 204.4 ($-\text{S}_2\text{CN}=$); 67.6, 65.9 (38)** (1 : 1, $=\text{NCH}_2-$), 29.3, 28.1, 27.3 (1 : 3 : 1, $=\text{CH}-$); 23.6, 22.7, 22.3, 21.9 (1 : 3 : 3 : 1, $-\text{CH}_3$).

Synthesis of complex I. Polymeric bis(*N,N*-diisobutylidithiocarbamato-*S,S*)gold(III) tetrachlorothallate(III) (compound **I**) was obtained by a reaction of freshly precipitated complex **II** with a solution of gold(III) chloride in 2 M HCl as follows. A solution of AuCl_3 in 2 M HCl (10 mL, gold amount 40.2 mg) was added to polymeric thallium(I) diisobutylidithiocarbamate (100 mg). The resulting mixture was stirred for 1 h. (The residual gold content of the solutions was determined by atomic absorption spectroscopy on a 180–50 instrument (Hitachi, class 1).) The yellow precipitate that formed was filtered off, washed with water, dried on the filter, and dissolved in acetone–ethanol (1 : 1). The powder dissolved incompletely leaving a gray precipitate, which was filtered off. The yellow mother liquor was used to grow transparent prismatic crystals of complex **I** for an X-ray diffraction experiment.

For complex **I**, ^{13}C MAS NMR, δ : 195.9, 194.3, 194.0, 191.8 (1 : 1 : 1 : 1, $-\text{S}_2\text{CN}=$); 61.1, 60.2, 58.8, 58.2 (2 : 2 : 2 : 2, $=\text{NCH}_2-$); 30.0, 29.0, 28.0, 27.5, 27.1 (1 : 1 : 2 : 1 : 3, $=\text{CH}-$); 22.3, 21.9, 21.5, 21.0, 20.7, 20.4, 20.2, 19.8 ppm (1 : 1 : 3 : 5 : 3 : 1 : 1 : 1 : $-\text{CH}_3$).

Scanning electron microscopy and electron-probe microanalysis. The degree of dispersion and morphology of samples of the undissolved precipitate were determined by high-resolution SEM on a JSM-35C JEOL analytical scanning electron microscope equipped with a 35-SDS wavelength-dispersive spectrometer. The secondary electron imaging mode was used to examine their morphology and microstructures. Qualitative determination of chemical elements in the samples was performed by electron-probe microanalysis on a RONTEC energy-dispersive spectrometer combined with a LEO-1420 scanning electron microscope.

^{13}C CP/MAS NMR spectra were recorded on a CMX-360 spectrometer (Agilent/Varian/Chemagnetics InfinityPlus) operating at 90.52 MHz (superconducting magnet with $B_0 = 8.46$ T; Fourier transform). The ^{13}C – ^1H cross polarization technique was used; ^{13}C – ^1H dipolar interactions were suppressed via proton decoupling in a magnetic field with the corresponding proton resonance frequency [16]. A sample (~50 mg) of complex **I** was packed into a 4.0-mm

ceramic (ZrO_2) rotor. The spinning rate in ^{13}C MAS NMR experiments was 5100(1) Hz. The number of scans was 2000. The proton $\pi/2$ -pulse duration was 5.0 μs . The ^{13}C – ^1H contact time was 2.5 ms; the pulses were spaced apart at 3.0 s. Isotropic ^{13}C chemical shifts δ (ppm) are referenced to a line of crystalline adamantane used as an external standard (δ 38.48 ppm relative to tetramethylsilane).

X-ray diffraction study was carried out at 120(2) K for prismatic single crystals of complex **I** on a Bruker-Nonius X8 Apex CCD diffractometer (MoK_α radiation, $\lambda = 0.71073$ Å, graphite monochromator). Crystallographic data were collected according to a standard procedure (ϕ and ω scan modes with small scan steps). An absorption correction was applied empirically (SADABS) [17]. Structure **I** was solved by the direct method and refined anisotropically (for non-hydrogen atoms) by the full-matrix least-squares method on F^2 . The hydrogen atoms were located geometrically and refined using a riding model. The residual electron density was within the expected range (-2.47 and $3.12\text{ e}/\text{\AA}^3$). All calculations for structure determination and refinement were performed with the SHELXTL program package [17]. Selected crystallographic parameters and the data collection and refinement statistics for structure **I** are given in Table 1. Bond lengths and bond angles in structure **I** are listed in Table 2.

Atomic coordinates, bond lengths, and bond angles for structure **I** have been deposited with the Cambridge Structural Database (no. 1009388; deposit@ccdc.cam.ac.uk or <http://www.ccdc.cam.ac.uk>).

The thermal behavior of complex I was studied by simultaneous thermal analysis involving parallel recording of TG and DSC curves. This study was carried out on an STA 449C Jupiter instrument (NETZSCH) in corundum crucibles. An opening in the cap of each crucible was provided to ensure a vapor pressure of 1 atm during thermolysis of a sample. A sample (3.043–6.142 mg) was heated under argon to 1100°C at a heating rate of 5°C/min. The temperature measurement accuracy was $\pm 0.7^\circ\text{C}$; the weight measurement accuracy was $\pm 1 \times 10^{-4}$ mg. TG and DSC curves were recorded using a correction file as well as temperature and sensitivity calibration data for a given temperature control program and a given heating rate. The melting temperature of complex **I** was independently determined on a PTP(M) instrument (OAO Khimlaborpribor).

RESULTS AND DISCUSSION

A reaction of complex **II** with a solution of AuCl_3 in 2 M HCl resulted in re-formation of the precipitate of the starting complex, its original white color turning light yellow with gradual deepening to yellow; therefore, the system under study produced new compounds. The above processes were accompanied by

* According to TG data, the original salt exists as trihydrate.

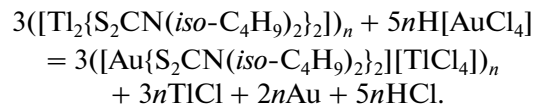
** Asymmetric ^{13}C – ^{14}N doublet (in Hz).

Table 1. Crystallographic parameters and the data collection and refinement statistics for structure **I**

Parameter	Value
Empirical formula	$C_{18}H_{36}N_2S_4Cl_4AuTl$
<i>M</i>	951.86
Crystal system	Monoclinic
Space group	$P2_1/n$
<i>a</i> , Å	15.6972(8)
<i>b</i> , Å	14.9821(8)
<i>c</i> , Å	26.1707(14)
β , deg	95.780(2)
<i>V</i> , Å ³	6123.5(6)
<i>Z</i>	8
ρ (calcd.), g/cm ³	2.065
μ , mm ⁻¹	10.675
<i>F</i> (000)	3600
Crystal dimensions, mm	0.58 × 0.10 × 0.06
θ Scan range, deg	1.57–30.07
Ranges of <i>h</i> , <i>k</i> , and <i>l</i> indices	$-22 \leq h \leq 22$, $-15 \leq k \leq 21$, $-36 \leq l \leq 33$
Number of measured reflections	36613
Number of unique reflections (R_{int})	17820 (0.0664)
Number of reflections with $I > 2\sigma(I)$	11140
Number of parameters refined	560
GOOF	0.939
<i>R</i> factors for $F^2 > 2\sigma(F^2)$	$R_I = 0.0502$, $wR_2 = 0.0913$
<i>R</i> factors for all reflections	$R_I = 0.1040$, $wR_2 = 0.1027$
Residual electron density (min/max), $e \text{ Å}^{-3}$	-2.471/3.117

decoloration of the working solution. The degree of gold binding was 95.3%.

Chemisorption of gold(III) from its solution with polymeric complex **II** involves ion exchange and a redox process. The tetrachloroaurate ion $[\text{AuCl}_4]^-$ as an oxidant ($[\text{AuCl}_4]^- + 3\bar{e} = \text{Au}^0 + 4\text{Cl}^-$, $E^0 = 1.000 \text{ V}$ [18]) can oxidize Tl^+ to Tl^{3+} ($\text{Tl}^+ + 4\text{Cl}^- - 2\bar{e} = [\text{TlCl}_4]^-$, $E^0 = 0.786 \text{ V}$ [19]), thereby reducing itself to metallic gold. Therefore, the heterogeneous reaction under discussion can be written as follows:



The reaction products were separated by dissolving them in acetone–ethanol (1 : 1). The major reaction product (complex **I**) is soluble in a mixture of organic solvents (see Experimental, under Synthesis of complex **I**). Other reaction products are TlCl and Au , which are insoluble in either water or organic solvents and form a fine heterogeneous powder (SEM image, Fig. 1a). Analysis of the energy-dispersive spectra (Figs. 1b, 1c) shows that the faintly colored areas are mainly contributed by thallium(I) chloride, while the darker ones represent reduced gold (see Fig. 1a).

The ^{13}C MAS NMR spectrum (Fig. 2) of complex **I** isolated from the chemisorption system under study contain resonance signals of the $=\text{NC(S)S}-$, $=\text{NCH}_2-$, $=\text{CH}-$, and $-\text{CH}_3$ groups (see Experimental, under Synthesis of complex **I**). Fragment-by-fragment modeling of the spectrum allowed distinguishing between the ^{13}C NMR signals from four non-equivalent $=\text{NC(S)S}-$ groups (1 : 1 : 1 : 1), which suggests a complicated structure of complex **I**.

To verify these conclusions, we studied the molecular and supramolecular structures of complex **I** by single-crystal X-ray diffraction.

The unit cell of structure **I** comprises eight formula units (Fig. 3). The cationic portion contains three structurally nonequivalent complex cations $[\text{Au}\{\text{S}_2\text{CN(iso-C}_4\text{H}_9)_2\}_2]^+$; hereafter, the cations with the Au(1), Au(2), and Au(3) atoms are denoted A, B, and C, respectively (Fig. 4, Table 2). The anionic portion consists of two nonequivalent $[\text{TlCl}_4]^-$ anions with the Tl(1) and Tl(2) atoms. The $[\text{TlCl}_4]^-$ anions are not centrosymmetric; the metal atom is surrounded by four Cl atoms making a distorted tetrahedron (the sp^3 -hybridization state of the central thallium atom). The $\text{CITl}(1)\text{Cl}$ and $\text{CITl}(2)\text{Cl}$ angles range from 108.27° to 111.49° and from 105.57° to 110.81° , respectively (Table 2).

In each of the complex cations A, B, and C, the dithiocarbamate ligands show a nearly isobidentate coordination (the Au–S bond lengths vary in a relatively narrow range from 2.327 to 2.348 Å) producing two four-membered chelate rings $[\text{AuS}_2\text{C}]$ sharing the gold atom. These rings are small (Au…C 2.832–

Table 2. Selected bond lengths d , bond angles ω , and torsion angles φ in structure I*

Bond	$d, \text{\AA}$	Bond	$d, \text{\AA}$
		Cation A	
Au(1)–S(11)	2.341(2)	S(12)–C(1)	1.741(8)
Au(1)–S(12)	2.336(2)	N(1)–C(1)	1.308(9)
Au(1)…S(24)	3.597(2)	N(1)–C(2)	1.467(9)
S(11)–C(1)	1.724(8)	N(1)–C(6)	1.478(10)
		Cation B	
Au(2)–S(21)	2.328(2)	S(23)–C(19)	1.754(7)
Au(2)–S(22)	2.327(2)	S(24)–C(19)	1.736(8)
Au(2)–S(23)	2.343(2)	N(2)–C(10)	1.289(10)
Au(2)–S(24)	2.348(2)	N(2)–C(11)	1.478(10)
Au(2)…S(11) ^a	3.718(2)	N(2)–C(15)	1.484(9)
Au(2)…S(32)	3.682(2)	N(3)–C(19)	1.298(9)
S(21)–C(10)	1.755(7)	N(3)–C(20)	1.462(9)
S(22)–C(10)	1.716(8)	N(3)–C(24)	1.467(9)
		Cation C	
Au(3)–S(31)	2.338(2)	S(32)–C(28)	1.736(7)
Au(3)–S(32)	2.338(2)	N(4)–C(28)	1.302(9)
Au(3)…S(23)	3.583(2)	N(4)–C(29)	1.464(9)
S(31)–C(28)	1.741(8)	N(4)–C(33)	1.458(10)
		Anion Tl(1)	
Tl(1)–Cl(11)	2.400(2)	Tl(1)–Cl(13)	2.398(2)
Tl(1)–Cl(12)	2.396(2)	Tl(1)–Cl(14)	2.416(3)
		Anion Tl(2)	
Tl(2)–Cl(21)	2.400(2)	Tl(2)–Cl(23)	2.406(2)
Tl(2)–Cl(22)	2.395(2)	Tl(2)–Cl(24)	2.391(2)
Angle	ω, deg	Angle	ω, deg
		Cation A	
S(11)Au(1)S(12)	75.14(7)	Au(1)S(12)C(1)	86.7(3)
S(11)Au(1)S(12) ^a	104.86(7)	S(11)C(1)S(12)	110.8(4)
Au(1)S(11)C(1)	86.9(3)		
		Cation B	
S(21)Au(2)S(22)	75.13(7)	Au(2)S(21)C(10)	87.1(3)
S(21)Au(2)S(23)	176.44(7)	Au(2)S(22)C(10)	88.0(3)
S(21)Au(2)S(24)	105.69(7)	Au(2)S(23)C(19)	87.4(3)
S(22)Au(2)S(23)	104.30(7)	Au(2)S(24)C(19)	87.6(2)
S(22)Au(2)S(24)	177.51(7)	S(21)C(10)S(22)	109.7(4)
S(23)Au(2)S(24)	75.03(7)	S(23)C(19)S(24)	109.9(4)
		Cation C	
S(31)Au(3)S(32)	75.12(7)	Au(3)S(32)C(28)	87.3(3)
S(31)Au(3)S(32) ^b	104.88(7)	S(31)C(28)S(32)	110.2(4)
Au(3)S(31)C(28)	87.1(3)		
		Anion Tl(1)	
Cl(11)Tl(1)Cl(12)	109.21(8)	Cl(12)Tl(1)Cl(13)	110.22(7)
Cl(11)Tl(1)Cl(13)	108.78(8)	Cl(12)Tl(1)Cl(14)	108.27(9)
Cl(11)Tl(1)Cl(14)	111.49(10)	Cl(13)Tl(1)Cl(14)	108.88(10)
		Anion Tl(2)	
Cl(21)Tl(2)Cl(22)	110.81(7)	Cl(22)Tl(2)Cl(23)	110.72(8)
Cl(21)Tl(2)Cl(23)	105.57(7)	Cl(22)Tl(2)Cl(24)	110.25(9)
Cl(21)Tl(2)Cl(24)	109.85(7)	Cl(23)Tl(2)Cl(24)	109.53(9)

Table 2. (Contd.)

Angle	ϕ , deg	Angle	ϕ , deg
Cation A			
Au(1)S(11)S(12)C(1)	-173.2(5)	S(11)C(1)N(1)C(6)	180.0(6)
S(11)Au(1)C(1)S(12)	-173.9(4)	S(12)C(1)N(1)C(2)	-175.9(6)
S(11)C(1)N(1)C(2)	3(1)	S(12)C(1)N(1)C(6)	1(1)
Cation B			
Au(2)S(21)S(22)C(10)	-179.4(4)	S(22)C(10)N(2)C(11)	170.2(6)
Au(2)S(23)S(24)C(19)	177.5(4)	S(22)C(10)N(2)C(15)	-7(1)
S(21)Au(2)C(10)S(22)	-179.5(4)	S(23)C(19)N(3)C(20)	-5(1)
S(23)Au(2)C(19)S(24)	177.7(4)	S(23)C(19)N(3)C(24)	178.7(5)
S(21)C(10)N(2)C(11)	-8(1)	S(24)C(19)N(3)C(20)	175.0(5)
S(21)C(10)N(2)C(15)	173.8(5)	S(24)C(19)N(3)C(20)	-1(1)
Cation C			
Au(3)S(31)S(32)C(28)	-173.9(4)	S(31)C(28)N(4)C(33)	173.1(5)
S(31)Au(3)C(28)S(32)	-174.5(4)	S(32)C(28)N(4)C(29)	178.9(5)
S(31)C(28)N(4)C(29)	-2(1)	S(32)C(28)N(4)C(33)	-5(1)

* The symmetry operation codes are: ^a $-x, 1-y, -z$; ^b $1-x, 1-y, -z$.

2.863 Å and S···S 2.838–2.857 Å). These interatomic distances are substantially shorter than the sum of the van der Waals radii of the gold and carbon atoms as well as than the van der Waals double radius of the sulfur atom (3.36 and 3.60 Å [20–22]). The fact that the gold and carbon atoms come so close to each other can be explained by their *trans*-annular interaction directly through the space of the chelate rings rather than through the bond system and by a high π -electron density within each ring. The chelate rings [AuS₂C] in cations A and C show some tetrahedral distortion: the torsion angles AuSSC and SAuCS appreciably deviate from 180° (Table 2). The diagonal angles SAuS in the chromophores [AuS₄] are or approach 180°, which suggests their square structure due to the low-spin inner-orbital dsp^2 -hybrid state of gold(III).

The fragments C₂NC(S)S in the dithiocarbamate ligands are virtually planar (the torsion angles SCNC are close to 180° or 0°, Table 2), and the N–C(S)S bonds (1.289–1.308 Å) are much stronger than the N–CH₂ bonds (1.458–1.484 Å). Both these facts suggest some contribution of double bonding to the formally single bond (i.e., mixing of the sp^2 - and sp^3 -

hybridization states of the N and C atoms in the fragment Dtc).

Although the complex cations A, B, and C are structurally similar, two distinctions between them should be noted: (a) cations A and C are centrosymmetric, while the acentric cation B contains two non-equivalent ligands Dtc (the presence of four nonequivalent dithiocarbamate ligands fully agree with the ¹³C MAS NMR data discussed above); (b) the Dtc ligands in cations A and C are bound with equal strength, in contrast to cation B showing reliably different bond strengths (2.327, 2.328 and 2.343, 2.348 Å). The aforementioned distinctions between cations A, B, and C in conjunction with their structural similarity enable them to be regarded as conformers. Earlier, we have already reported on conformational isomerism in dialkyldithiocarbamate complexes (e.g., see [23–30]).

Further (supramolecular) structural self-organization of complex I involves pairs of relatively weak secondary nonvalent Au···S bonds between isomeric gold(III) cations (Fig. 5). These bonds form zigzag polymer chains (...A···B···C···B...)_n with alternating nonequivalent cations A, B, and C (1:2:1). The angle Au(1)Au(2)Au(3) is 159.25°; the angles

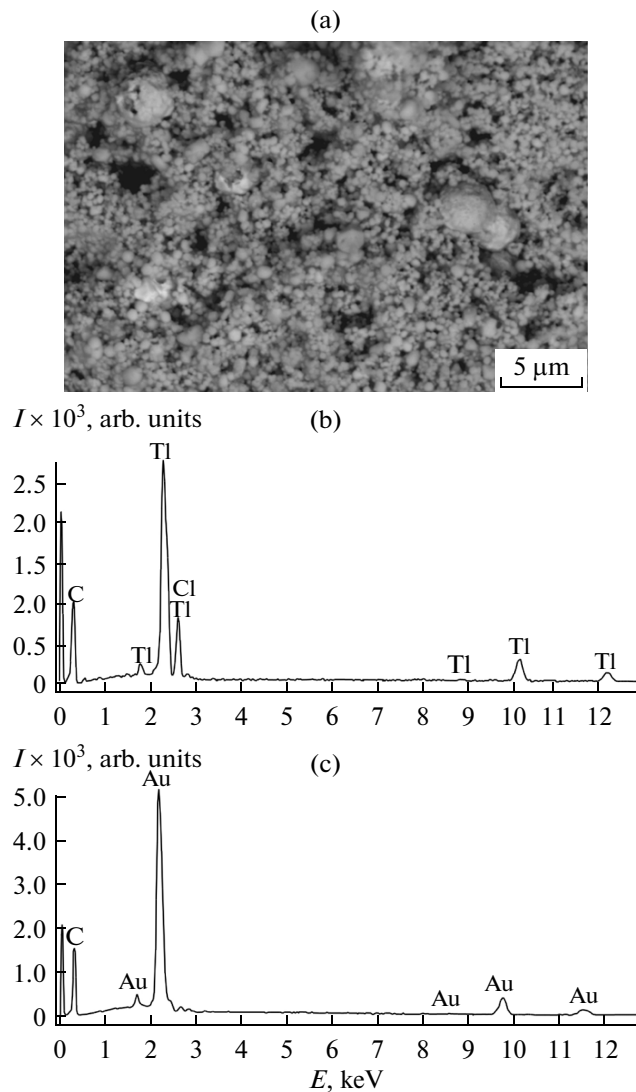


Fig. 1. (a) Particle size and shape for the insoluble precipitate; the energy-dispersive spectra revealing the presence of (b) TlCl and (c) reduced gold.

$\text{Au}(2)\text{Au}(1)\text{Au}(2)$ and $\text{Au}(2)\text{Au}(3)\text{Au}(2)$ are both 180° . Nonequivalent $[\text{TlCl}_4]^-$ anions are on both sides of the polymer chains (Fig. 3). It can be seen in the structural fragment shown in Fig. 5 that isomeric complex gold(III) cations differently interact with each other when forming a polymeric chain. In the chain under consideration, each of the centrosymmetric cations A and C is surrounded by two acentric cations B and linked to them by two pairs of unsymmetrical secondary $\text{Au} \cdots \text{S}$ bonds: $\text{Au}(1) \cdots \text{S}(24)$ 3.597 Å; $\text{S}(11)^a \cdots \text{Au}(2)$ 3.718 Å for cation A and $\text{Au}(3) \cdots \text{S}(23)$ 3.583 Å; $\text{S}(32) \cdots \text{Au}(2)$ 3.682 Å for cation C. All the interatomic distances $\text{Au} \cdots \text{S}$ appreciably exceed the sum of the van der Waals radii of the gold and sulfur atoms (3.46 Å [20–22]). It should be noted that in cations A and C, the bonds under discussion involve gold atoms and diagonally oriented sulfur atoms (S(11), S(11)^a and S(32), S(32)^b). In cation B, nonvalent

bonds are formed by the $\text{Au}(2)$ atom and both sulfur atoms (S(23) and S(24)) of only one nonequivalent dithiocarbamate ligand. Such an asymmetric character of interactions between the cations accounts for somewhat different distances between the adjacent gold atoms ($\text{Au}(1) \cdots \text{Au}(2)$ 4.022 Å; $\text{Au}(2) \cdots \text{Au}(3)$ 3.957 Å).

The thermal behavior of complex I was studied by simultaneous thermal analysis involving parallel recording of TG and DSC curves. The TG curve reveals two steps of the thermolysis (Fig. 6a). The first step (143–295°C) is due to thermal decomposition of the dithiocarbamate portion of complex I and the $[\text{TlCl}_4]^-$ anions; this is accompanied by reduction of gold to the metallic state and by release of thallium(I) chloride. (Above 150°C TlCl_3 decomposes into TlCl and Cl_2 [31].) The experimental weight loss (52.46%) in the first step is somewhat lower than the calculated

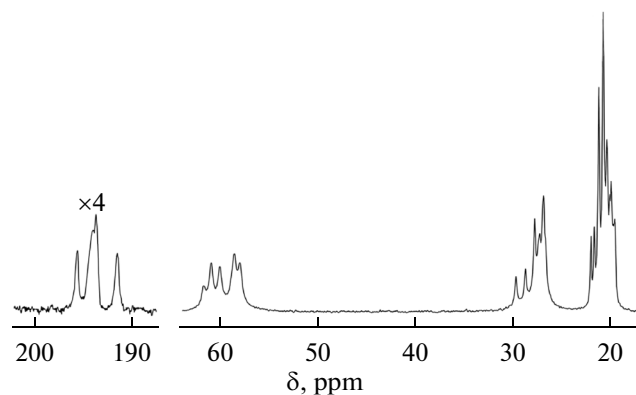


Fig. 2. ^{13}C MAS NMR spectrum of polycrystalline complex I. The number of scans/spinning frequency (Hz) is 2000/5100.

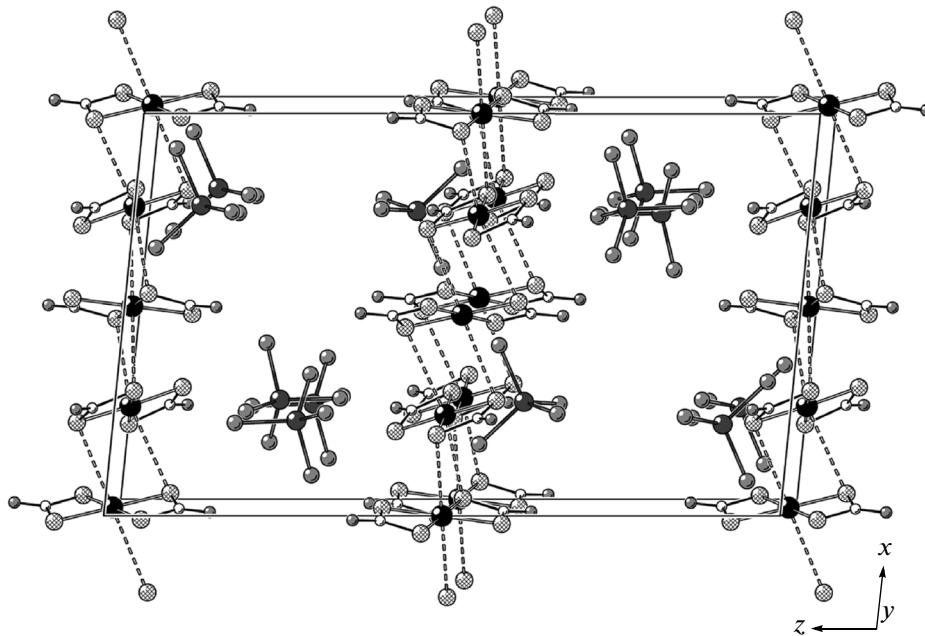


Fig. 3. Crystal packing for structure I (projection onto the plane xz).

value (54.11%). The second step (295–550°C) occurring by evaporation of TiCl is characterized by a weight loss of 23.21% (calc. 25.20%). The segment of the TG curve from ~550 to ~800°C is associated with completion of the desorption of volatile thermolysis products. The weight of the residue at 1100°C is 21.66% of the weight of the initial complex, which is somewhat higher than the value (20.69%) calculated for reduced metallic gold. After completion of the thermolysis, small beads of gold were found on the bottom of the crucible (Fig. 6c).

The DSC curve shows a number of endothermic peaks (Fig. 6b). Two low-temperature peaks at 149.5 and 261.1°C are due to melting of the sample (extrapolated m.p. 144.8°C; an independent measurement in

a glass capillary gave m.p. 145°C) and intense thermal decomposition of complex I (corresponding to the first step in the TG curve), respectively. Another weak endothermic peak at 423°C should be attributed to melting of TiCl contaminated with thermolysis products (m.p. 431°C [31]). The high-temperature region features an endothermic peak due to melting of gold (extrapolated m.p. 1061.4°C).

ACKNOWLEDGMENTS

We are grateful to O.N. Antsutkin (Luleå University of Technology, Luleå, Sweden) for providing the facilities for ^{13}C MAS NMR experiments.

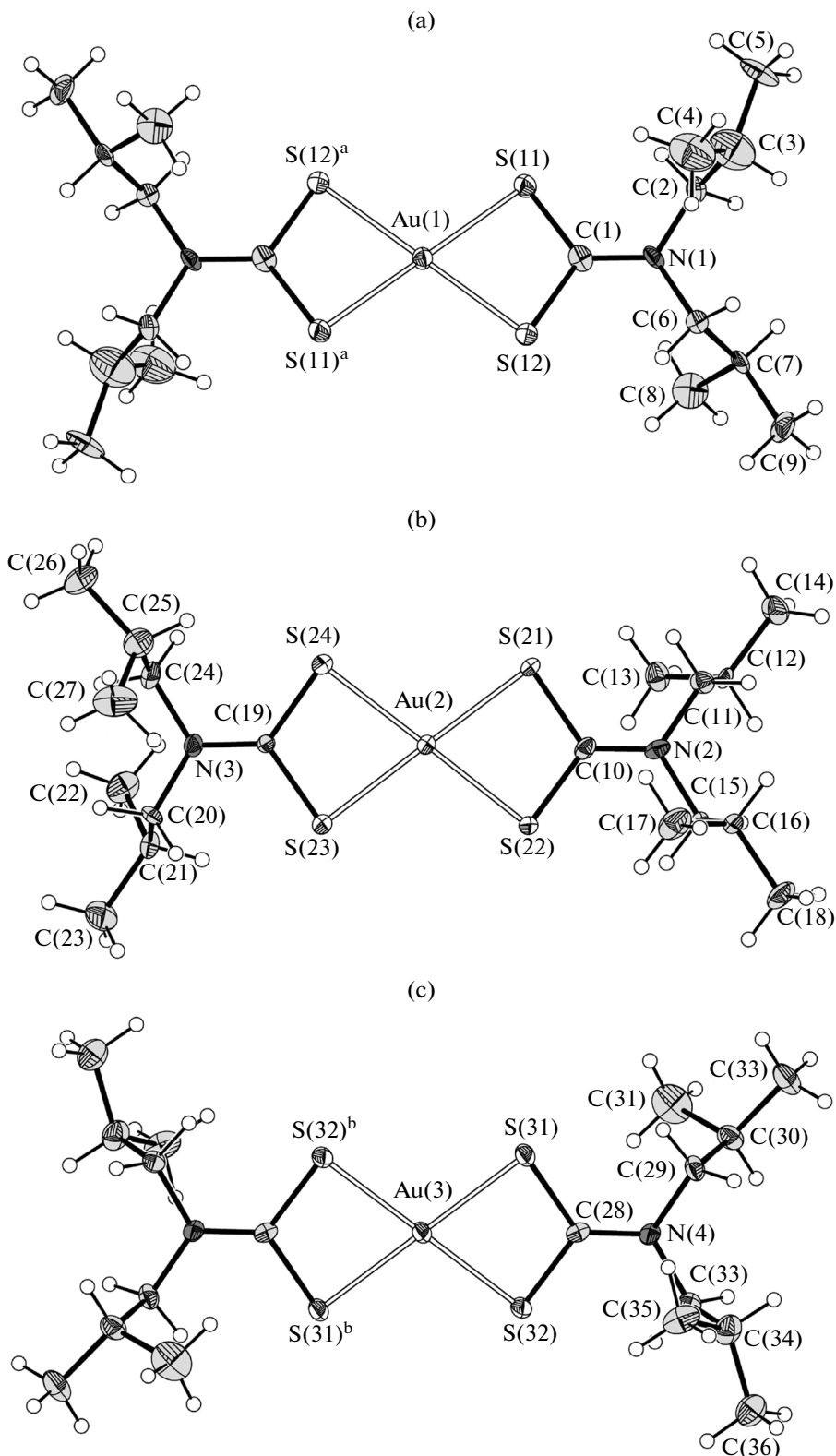


Fig. 4. Isomeric complex cations (a) A, (b) B, and (c) C with atomic displacement ellipsoids (50% probability).

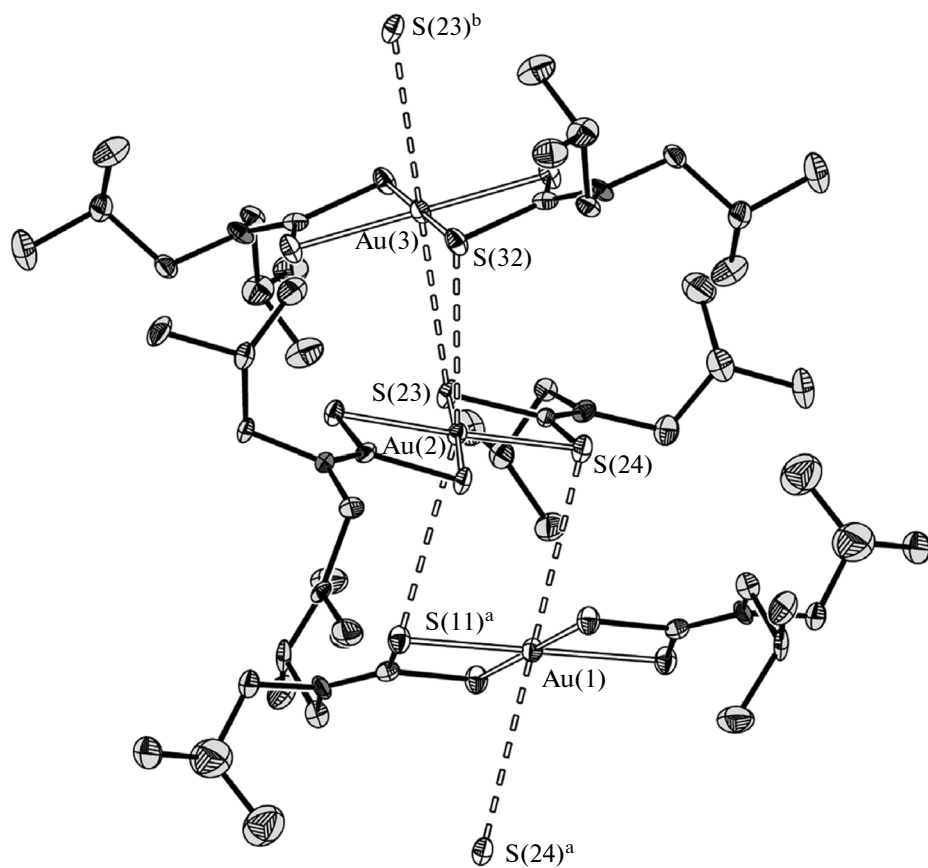


Fig. 5. Three-unit structural fragment of the polymeric chain.

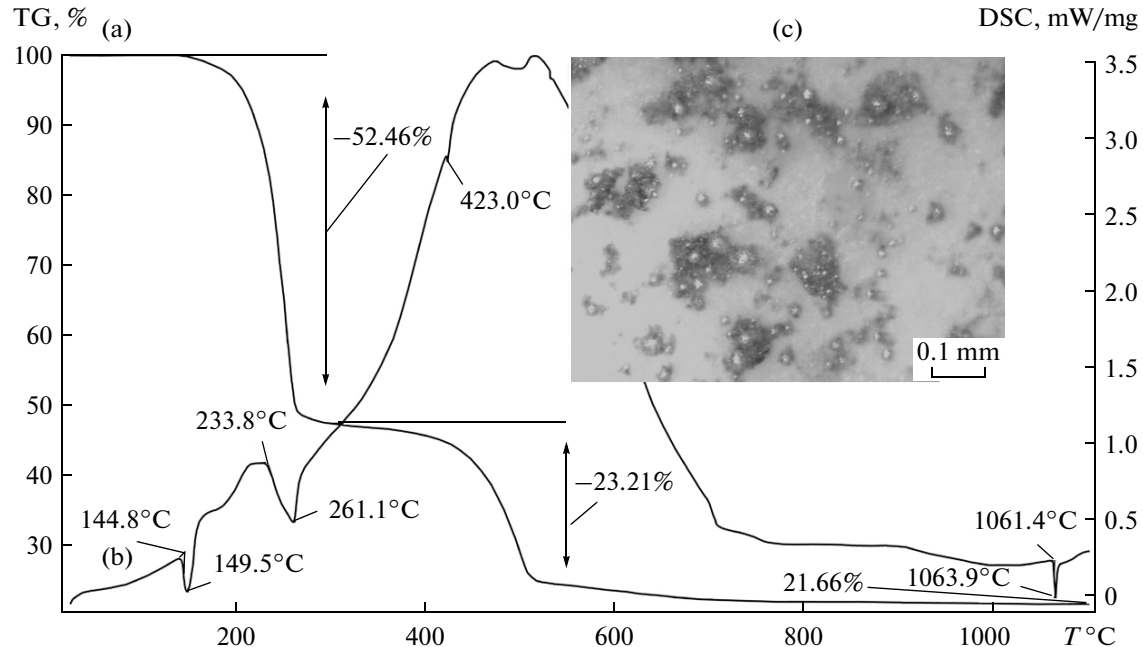


Fig. 6. (a) TG and (b) DSC curves of complex I. (c) A close-up view of the bottom of the crucible containing gold beads above m.p.

This study was supported in part by the Presidium of the Russian Academy of Sciences (Basic Research Program “Development of Methods for the Synthesis of Chemical Compounds and for the Design of Novel Materials”) and the Presidium of the Far East Branch of the Russian Academy of Sciences (project nos. 12-I-P8-01 and 12-III-A-04-040).

REFERENCES

1. Byr'ko, V.M., *Ditiokarbamaty* (Dithiocarbamates), Moscow: Nauka, 1984.
2. Anacker-Eickhoff, H., Jennische, P., and Hesse, R., *Acta Chem. Scand.*, 1975, vol. A29, no. 1, p. 51.
3. Alexander, N., Ramalingam, K., and Rizzoli, C., *Inorg. Chim. Acta*, 2011, vol. 365, no. 1, p. 480.
4. Ramalingam, K., Alexander, N., and Rizzoli, C., *Monatsh. Chem.*, 2013, vol. 144, no. 9, p. 1329.
5. Akhbari, K. and Morsali, A., *Coord. Chem. Rev.*, 2010, vol. 254, nos. 17–18, p. 1977.
6. Ivanov, A.V., Bredyuk, O.A., Gerasimenko, A.V., et al., *Russ. J. Coord. Chem.*, 2006, vol. 32, no. 5, p. 339.
7. Ivanov, A.V., Bredyuk, O.A., Gerasimenko, A.V., and Antzutkin, O.N., *Dokl. Phys. Chem.*, 2008, vol. 420, no. 2, p. 130.
8. Rodina, T.A., Ivanov, A.V., Bredyuk, O.A., and Gerasimenko, A.V., *Russ. J. Coord. Chem.*, 2009, vol. 35, no. 3, p. 170.
9. Sivagurunathan, G.S., Ramalingam, K., and Rizzoli, C., *Polyhedron*, 2013, vol. 65, p. 316.
10. Rodina, T.A., Ivanov, A.V., Loseva, O.V., and Bredyuk, O.A., *Russ. J. Inorg. Chem.*, 2009, vol. 54, no. 12, p. 1964.
11. Ivanov, A.V., Loseva, O.V., Gerasimenko, A.V., and Sergienko, V.I., *Dokl. Phys. Chem.*, 2009, vol. 426, no. 1, p. 92.
12. Rodina, T.A., Ivanov, A.V., Gerasimenko, A.V., et al., *Polyhedron*, 2012, vol. 40, no. 1, p. 53.
13. Loseva, O.V., Rodina, T.A., Ivanov, A.V., et al., *J. Struct. Chem.*, 2013, vol. 54, no. 3, p. 598.
14. Loseva, O.V., Rodina, T.A., and Ivanov, A.V., *Russ. J. Coord. Chem.*, 2013, vol. 39, no. 6, p. 463.
15. Ivanov, A.V., Loseva, O.V., Rodina, T.A., et al., *Russ. J. Inorg. Chem.*, 2014, vol. 59, no. 8, p. 807.
16. Pines, A., Gibby, M.G., and Waugh, J.S., *J. Chem. Phys.*, 1972, vol. 56, no. 4, p. 1776.
17. APEX2 (version 1.08), SAINT (version 7.03), SADABS (version 2.11) and SHELXTL (version 6.12), Madison (WI, USA): Bruker AXS Inc., 2004.
18. Belevantsev, V.I., Peshchevitskii, B.I., and Zemskov, S.V., *Izv. Sib. Otd. Akad. Nauk SSSR. Ser. Khim.*, 1976, no. 4(2), p. 24.
19. Lidin, R.A., Andreeva, L.L., and Molochko, V.A., *Spravochnik po neorganicheskoi khimii* (Handbook in Inorganic Chemistry), Moscow: Khimiya, 1987.
20. Pauling, L., *The Nature of the Chemical Bond and the Structure of Molecules and Crystals*, London: Cornell Univ., 1960.
21. Bondi, A., *J. Phys. Chem.*, 1964, vol. 68, no. 2, p. 441.
22. Bondi, A., *J. Phys. Chem.*, 1966, vol. 70, no. 9, p. 3006.
23. Ivanov, A.V. and Antzutkin, O.N., *Top. Curr. Chem.*, 2005, vol. 246, p. 271.
24. Ivanov, A.V., Gerasimenko, A.V., Konzelko, A.A., et al., *Inorg. Chim. Acta*, 2006, vol. 359, no. 12, p. 3855.
25. Ivanov, A.V., Kritikos, M., Antzutkin, O.N., and Forsling, W., *Inorg. Chim. Acta*, 2001, vol. 321, nos. 1–2, p. 63.
26. Ivanov, A.V., Mitrofanova, V.I., Kritikos, M., and Antzutkin, O.N., *Polyhedron*, 1999, vol. 18, no. 15, p. 2069.
27. Ivanov, A.V., Pakusina, A.P., Ivanov, M.A., et al., *Dokl. Phys. Chem.*, 2005, vol. 401, no. 2, p. 44.
28. Sharutin, V.V., Ivanov, M.A., Gerasimenko, A.V., et al., *Russ. J. Coord. Chem.*, 2006, vol. 32, no. 6, p. 387.
29. Ivanov, A.V., Zaeva, A.S., Gerasimenko, A.V., and Forsling, V., *Dokl. Phys. Chem.*, 2005, vol. 404, no. 2, p. 205.
30. Ivanov, A.V., Zaeva, A.S., Novikova, E.V., et al., *Russ. J. Coord. Chem.*, 2007, vol. 33, no. 4, p. 233.
31. Lidin, R.A., Molochko, V.A., and Andreeva, L.L., *Khimicheskie svoistva neorganicheskikh veshchestv* (Chemical Properties of Inorganic Compounds), Moscow: Khimiya, 2000.

Translated by D. Tolkachev